8 Group III: Rotating-Drum and Stirred-Drum Bioreactors

David A. Mitchell, Deidre M. Stuart, Matthew T. Hardin, and Nadia Krieger

8.1 Introduction

This chapter addresses the design and operation of rotating-drum bioreactors and those stirred-drum bioreactors in which the air is blown into the headspace and not forcefully through the substrate bed itself. This type of bioreactor might be chosen for continuous processes, which will be discussed in Chap. 11. It can also be used for batch processes, which will be the focus of this chapter. Note that there are several bioreactors that are very similar in appearance to rotating- and stirred-drum bioreactors in which air is introduced directly into the bed. This forced aeration would tend to place them in the Group IVa bioreactors considered in Chap. 9 (continuously-agitated, forcefully-aerated bioreactors), however, whether the bioreactor performs more closely to this type of bioreactor or to a rotating-drum or stirred-drum bioreactor depends on the effectiveness of this forced aeration.

8.2 Basic Features, Design, and Operating Variables for Group III Bioreactors

The basic design features have already been presented in Sect. 3.3.1. Some possible design variations include (Fig. 8.1):

- the inclusion of baffles (or, more correctly, “lifters”);
- periodic reversal of the direction of rotation;
- use of drum cross-sections that are not circular;
- inclination of the drum axis to the horizontal.

Design variables for both baffled rotating-drum and stirred-drum bioreactors include (Fig. 8.2):

- the length and diameter of the bioreactor. Note that the geometric proportions can vary over quite a wide range;
- the inclination of the central axis of the bioreactor to the horizontal;

- the size and shape of the mixing device within a stirred-drum and the number, size, and shape of baffles in a baffled rotating-drum;
- the design of the inlet and outlet of the aeration system, which will affect the gas flow patterns in the headspace;
- the presence or absence of an external water jacket. Note that for a rotating drum this will increase the weight to be rotated and also will require a rotating water seal on the inlet and outlet water lines;
- whether internal features such as baffles or paddles are designed to aid in cooling;
- the design of the system for the addition of water or other additives to the bed during the process;
- in continuous operation, the design of the substrate inlet and outlet.

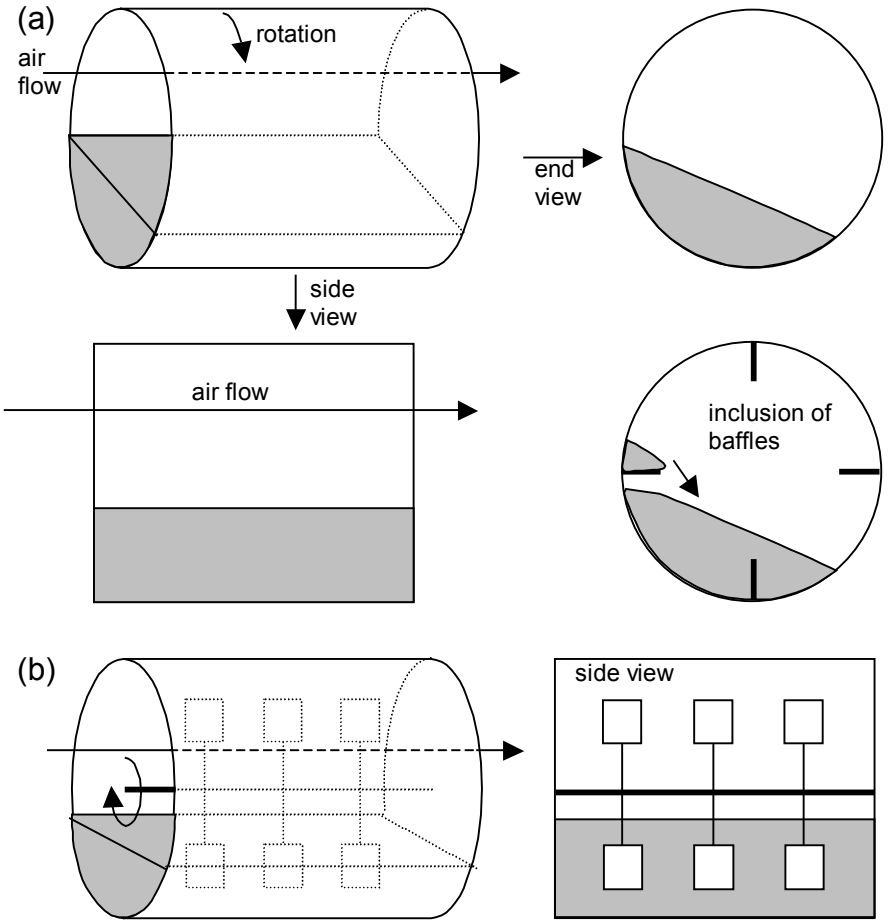

Fig. 8.1. Basic features of **(a)** rotating-drum bioreactors and **(b)** stirred-drum bioreactors

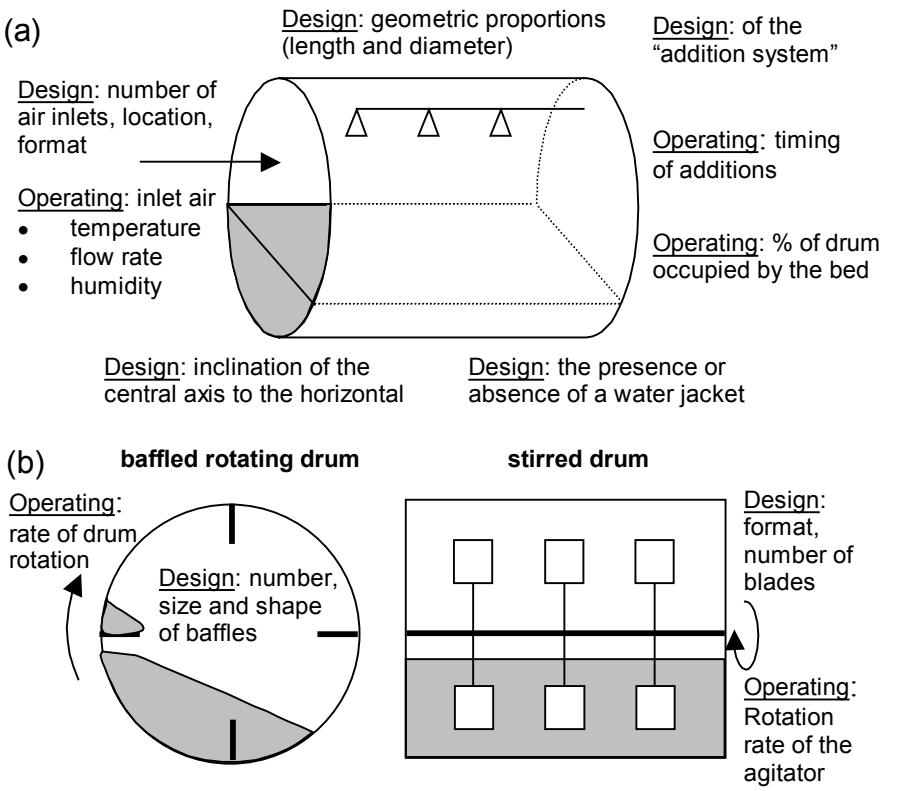

Fig. 8.2. Design and operating variables that are available with rotating-drum and stirred-drum bioreactors. **(a)** Design and operating variables that are the same for both types. **(b)** Design and operating variables that are specific for the bioreactor type

The operating variables that are available include (Fig. 8.2):

- the solids loading used;
- the rotational speed for a rotating-drum bioreactor, the stirring speed for a stirred-drum bioreactor. If rotation or stirring are done intermittently, then the frequency, duration, and speed of rotation or stirring events;
- the flow rate, temperature, and humidity of the air blown into the headspace;
- the timing of water additions;
- the temperature of the cooling water if a jacket is used; if a jacket is not used then whether air is forcefully blown past the drum wall or not.

Most of these operating variables can be changed at will during the fermentation. The solids loading is an operating variable that is fixed at the beginning of each run. Note that it does change during the fermentation as part of the solids is converted into CO_2, but once a fermentation has commenced, the solids loading

cannot be freely controlled. The solids loading is related to the "fractional filling" of the drum, that is, the fraction of the whole drum volume occupied by the bed, here represented by the symbol ω. Typically, fractional fillings should be kept below 0.4, in order to enable reasonable mixing of the bed.

Since the bed is mixed, water can be replenished by spraying a fine mist onto the bed during mixing. Therefore evaporation can be promoted as part of the cooling strategy, meaning that unsaturated air can be used at the air inlet.

The values chosen for the design and operating variables will be affected by the following considerations:

- the heat production rate in the bed will strongly influence decisions about the loading of the bioreactor, the aeration rate, and the humidity of the inlet air.
- the rotation rate or stirring speed chosen will represent a balance between the promotion of heat and O_2 transfer within the bed and between the bed and the headspace and the minimization of shear damage to the microorganism.
- the strength of the particles may affect the maximum diameter and the substrate loading that can be used. Soft particles may be crushed by the weight of a large overlying bed.

This chapter explains what is known, on the basis of experimental studies, about how these design and operating variables influence the performance of rotating-drum bioreactors and stirred-drum bioreactors. Chapter 23 shows how mathematical models can be used to explore further the design and operation of rotating-drum and stirred-drum bioreactors.

8.3 Experimental Insights into the Operation of Group III Bioreactors

8.3.1 Large-Scale Applications

Takamine (1914) developed a process for the production of amylase by *Aspergillus oryzae* on wheat bran, first in tray bioreactors and then later in rotating-drum bioreactors. This work was later extended by Underkofler et al. (1939). Ziffer (1988) was involved in work during the early 1940s in which penicillin was produced at commercial scale by SSF of wheat bran, in a plant containing 40 rotating-drum bioreactors of 1.22 m diameter and 11.28 m length, meaning that each bioreactor had a total volume of 13 m^3 (Fig. 8.3(a)). He described how the system was operated, but not how it performed.

The bran was mixed with the nutrient solution externally and then added through the access hatches. These were closed and the bioreactor was sterilized by direct injection of steam, at 1 atm above ambient pressure, while being rotated at 24 rpm. Inoculum was added through spray nozzles, while the drum was rotating at 24 rpm. The aeration rate was maintained between 0.28 and 0.42 $m^3\ min^{-1}$

until 30 h, then it was increased to 1.13 m^3 min^{-1}, which was maintained until the end of the fermentation. The rotation rate was maintained at 24 rpm during the first 6 h. It was reduced to 5 rpm between 6 and 30 h and then increased to 24 rpm, which was maintained until the end of the fermentation. Water was sprayed onto the external surface in order to aid temperature control. At the end of the fermentation (112 h), the fermented substrate was removed through the access hatches by a pneumatic vacuum system.

Rotating-drum bioreactors have also been used in the *koji* industry. Sato and Sudo (1999) report the use of a rotating-drum bioreactor of 1500 kg capacity, which is designed to rotate intermittently (Fig. 8.3(b)). They report that accurate temperature control is difficult in this type of bioreactor, but provide no details.

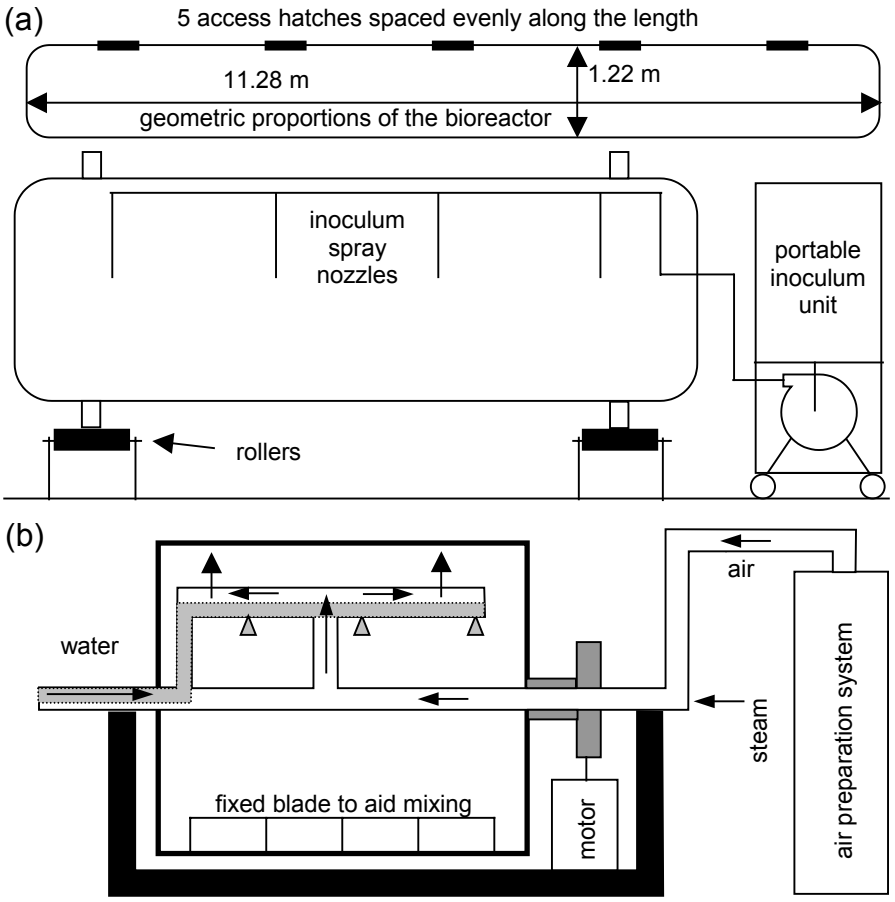

Fig. 8.3. Basic design features of large-scale rotating-drum bioreactors. **(a)** Drums used for penicillin production. This is a simplified version of a diagram presented by Ziffer (1988). **(b)** *Koji* bioreactor. This is a simplified version of a diagram presented by Sato and Sudo (1999)

8.3.2 Pilot-Scale Applications

Fung and Mitchell (1995) investigated the effect of the presence and absence of baffles on the performance of a 200-L rotating-drum bioreactor, in which *Rhizopus oligosporus* was grown on wheat bran. The drum had an internal diameter of 56 cm and an internal length of 85 cm. When baffles were used, four baffles of 17 cm width and 85 cm length were attached at right angles to the inner wall of the drum, with uniform spacing between them (i.e., in the manner indicated in Fig. 8.1). There was no external temperature control; the bioreactor operated within a room that varied from 17 to 26°C. Pre-humidified air was blown through the bioreactor at the optimum temperature for growth of the organism of 37°C.

The aeration at 37°C was not sufficient to maintain the bed temperature at a value suitable for initial growth. As a result, there was a long lag period, with bed temperatures below 30°C (Fig. 8.4(a)). This was especially true for the baffled drum, for which heat transfer between the bed and surroundings was more efficient. In the unbaffled drum the temperature was slightly higher during the lag phase and, as a result, the lag phase was slightly shorter.

The temperature then increased, over a period of 10 h, to values around 45°C. In the baffled drum the temperature then decreased quickly again. The bed was at temperatures of above 40°C for only 10 h. In the unbaffled bioreactor the temperature remained at values above 40°C for 30 h.

Peak O_2 consumption rates were higher in the baffled drum, as shown by the greater slope of the cumulative O_2 uptake profile in Fig. 8.4(a). However, due to the longer lag phase, the O_2 uptake was not significantly better in the baffled drum. Note that the baffled drum would have outperformed the unbaffled drum over the first 30 h, if the bed temperature in both drums had been maintained at 37°C during the first 10 h. This could be achieved with a water jacket or by placing the bioreactor in a 37°C room. Alternatively, it might be sufficient simply to insulate the outer surfaces of the bioreactor during the early stages of the fermentation, such that heating of the bed by the inlet air would be more efficient. Obviously, such insulation would need to be removed once rapid growth began.

These results, obtained at pilot scale, demonstrate a major challenge to be overcome in rotating-drum bioreactors, namely the adequate removal of the waste metabolic heat from the substrate. For example, in the fermentations described above that were undertaken with *R. oligosporus*, it was highly desirable to avoid temperatures above 40°C, but this value was exceeded for long periods.

Stuart (1996) grew *Aspergillus oryzae* on wheat bran in the same 200-L bioreactor, without baffles. Performance in terms of O_2 consumption was significantly better at 9 rpm than at 2 rpm (Fig. 8.4(b)). This is most likely due to the effect of the rotational speed on the effectiveness of the mixing within the bed. At 2 rpm the bed slumped within the bioreactor while at 9 rpm there was a tumbling flow regime (flow regimes in unbaffled rotating-drum bioreactors are discussed in more detail in Sect. 8.4.1). The maximum temperatures reached during the fermentations were about 43°C at 9 rpm and about 38°C at 2 rpm. The higher temperature occurred at the higher rotational rate due to better mixing, which allowed better O_2 transfer from the headspace into the bed, which in turn allowed faster growth.

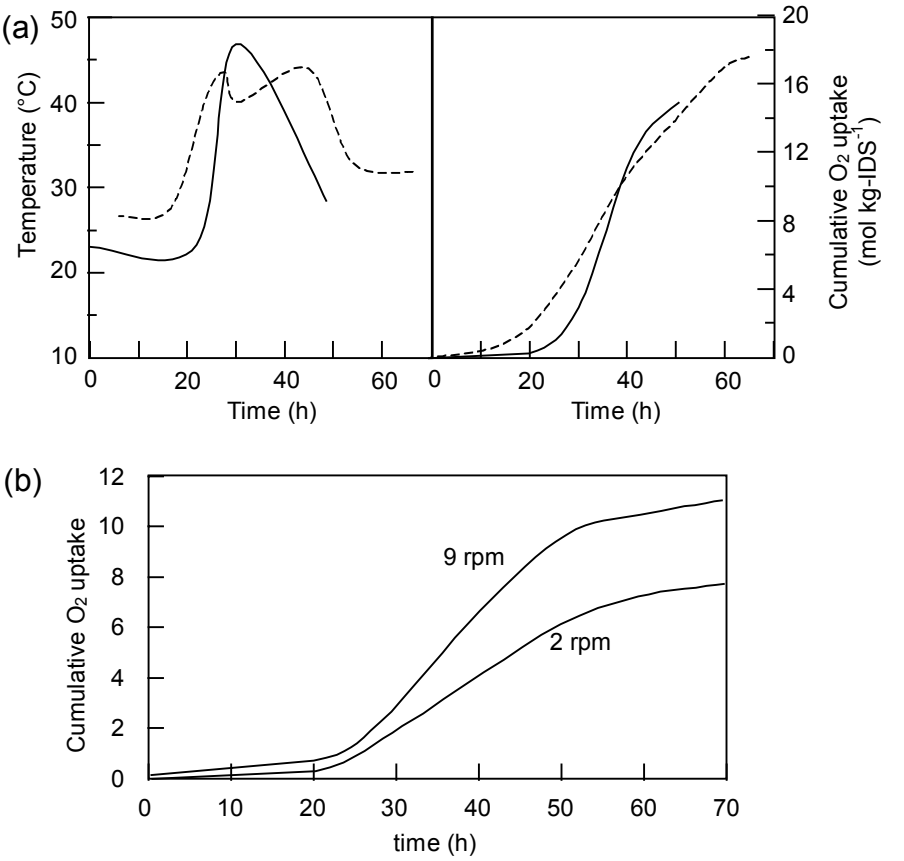

Fig. 8.4. (a) Effect of baffles on the performance of a 200-L rotating-drum bioreactor. Adapted from Fung and Mitchell (1995) with kind permission of Springer Science and Business Media. Key: (- - -) unbaffled drum; (—) baffled drum. **(b)** Effect of rotation rate on the performance of an unbaffled 200-L rotating-drum bioreactor (Stuart 1996). IDS is "Initial Dry Solids"

8.3.3 Small-Scale Applications

Stuart et al. (1999) undertook studies in a bioreactor of 85 cm length and 19 cm internal diameter, giving a volume of approximately 20 L. The bioreactor was operated with various substrate loadings and rotational speeds. *Aspergillus oryzae* was used, in some cases grown on wheat bran, in others on an artificial gel substrate. The temperature in the chamber was maintained at 30-32°C and air was supplied at this temperature. Relevant observations were:

- **Regarding the effect of rotational speed on growth on the gel substrate.** Between 0 and 10 rpm, there was a beneficial effect of rotation, with an increase in the maximum specific growth rate, while the amount of protein enrichment

that occurred remained constant (Fig. 8.5). As the rotational speed used in the fermentation increased from 10 to 50 rpm, there were decreases in both the amount of protein enrichment obtained during the fermentation and the maximum specific growth rate observed.

- **Regarding the effect of the substrate used on the temperatures reached within the bed.** During fermentations with the gel substrate, the bed temperature did not exceed 35°C, while during fermentations with the wheat bran substrate the temperature peaked at values between 45 and 50°C. This effect is probably related to the availability of the carbon sources in the two substrates. The gel substrate contained slightly less than 5% starch by weight (on a wet basis) while the wheat bran substrate contained 15% starch by weight (on a wet basis) and in addition had protein and fat available. Also note that the majority of wheat bran particles were flat and smaller than 4 mm diameter while the gel substrate consisted of 6 mm cubes, such that the wheat bran substrate had a much larger surface area to volume ratio.

De Reu et al. (1993) built a rotating-drum bioreactor in which one end was fixed, in order to allow the insertion of sensors into the bed (Fig. 8.6(a)). This complicates the design, as it is necessary to have a seal between the rotating body and the fixed end-plate. The bioreactor had an inner diameter of 20 cm and a length of 15 cm, giving a total volume of 4.7 L. Although the bed volume was not specifically mentioned, fermentations were undertaken with 1 kg of cooked soybeans (inoculated with *Rhizopus oligosporus*), meaning that the bed volume was probably between 2 and 2.5 L. Air was introduced into the headspace through the central axis. The bioreactor was placed in a room with an air temperature of 30°C.

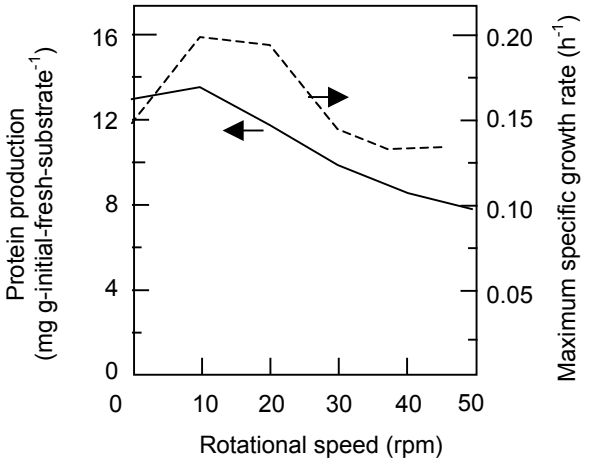

Fig. 8.5. Effect of rotational speed on the performance of a laboratory-scale rotating-drum bioreactor in which *Aspergillus oryzae* was grown on a gel-based artificial substrate. Key: (—) Amount of protein produced during the fermentation; (- - -) maximum value of the specific growth rate. Adapted from Stuart et al. (1999) with kind permission from John Wiley & Sons, Inc.

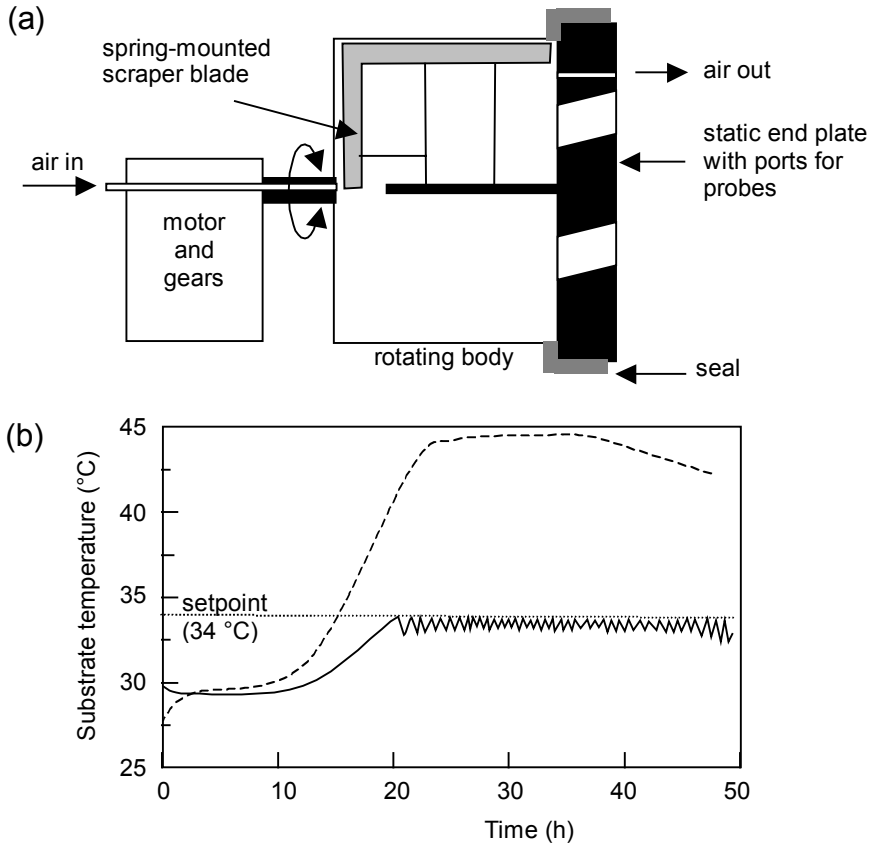

Fig. 8.6. Performance of a laboratory-scale rotating-drum bioreactor operated in a discontinuous agitation mode (de Reu et al. 1993). **(a)** Main features of the bioreactor used. **(b)** Control of bed temperature through the discontinuous rotation period. Key: (- - -) Temperature profile during a static fermentation; (—) Temperature profile during a discontinuously agitated fermentation. Adapted from de Reu et al. (1993) with kind permission of Springer Science and Business Media.

This bioreactor was used to investigate the use of discontinuous rotation for bed temperature control. Each time the bed temperature reached 34°C, a 60 s rotation period was triggered, with several clockwise and anticlockwise rotations, at rates of 4 to 6 rpm. Although it was possible to control the temperature of the 1-kg bed using this strategy (Fig. 8.6(b)), it is unlikely to be effective at large scale.

Kalogeris et al. (1999) developed a bioreactor that is a variation of a rotating-drum bioreactor (Fig. 8.7). In this bioreactor the substrate bed is held within a 10-L perforated cylinder that can be rotated. This perforated cylinder is inside a larger water-jacketed solid-walled cylinder through which air is passed. This bioreactor did work well for the cultivation of thermophilic organisms, but heat removal from the bed is unlikely to be sufficient for the cultivation of mesophiles,

for two reasons. Firstly, the air blown into the headspace region will preferentially flow past the surface of the bed rather than through the bed itself (it is for this reason that this bioreactor is classified as a group III bioreactor). Secondly, there is no intimate contact between the bed and the water jacket; a layer of process air separates them. This type of operation was later adapted for an SSF process in which a nutrient medium was placed in the bottom of the bioreactor and nylon sponge cubes were regularly wetted with this nutrient medium as the inner perforated drum rotated at 3 rpm (Dominguez et al. 2001). The system was used for ligninolytic enzyme production by *Phanerochaete chrysosporium*.

Roller bottle systems are useful for testing, at laboratory scale, a number of different treatments for a process intended to be performed in a rotating-drum bioreactor. Figure 8.8 indicates one possible way in which a roller system can be constructed. Note that the direct introduction of air into the headspace of each individual bottle is complicated, although not impossible. In the majority of cases it would be more likely for each bottle simply to have a perforated lid, with a passive exchange of gases between the headspace and the surrounding air.

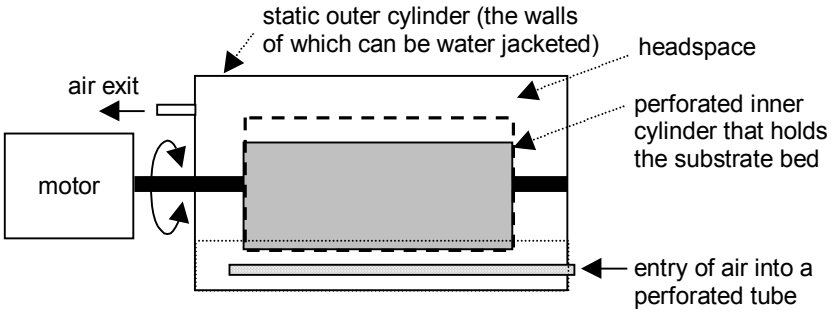

Fig. 8.7. General design principles of the Group III bioreactor used by Kalogeris et al. (1999) and Dominguez et al. (2001). The bottom of the bioreactor of Dominguez et al. (2001) was filled with a liquid nutrient medium up to the level shown by the dotted line. In the case of the bioreactor of Kalogeris et al. (1999) there was no liquid held by the outer cylinder. Adapted from Dominguez et al. (2001) with kind permission of Elsevier

8.4 Insights into Mixing and Transport Phenomena in Group III Bioreactors

The performance of rotating-drum and stirred-drum bioreactors will depend strongly on the effectiveness of the exchange of water and energy between the bed and the headspace gases. The effectiveness of this exchange will be affected by the flow patterns within the bed and headspace. It is unlikely that rotating- or stirred-drum bioreactors will be well mixed, unless specific attention is paid at the design stage to the promotion of mixing. Rather, air flow patterns and solids flow

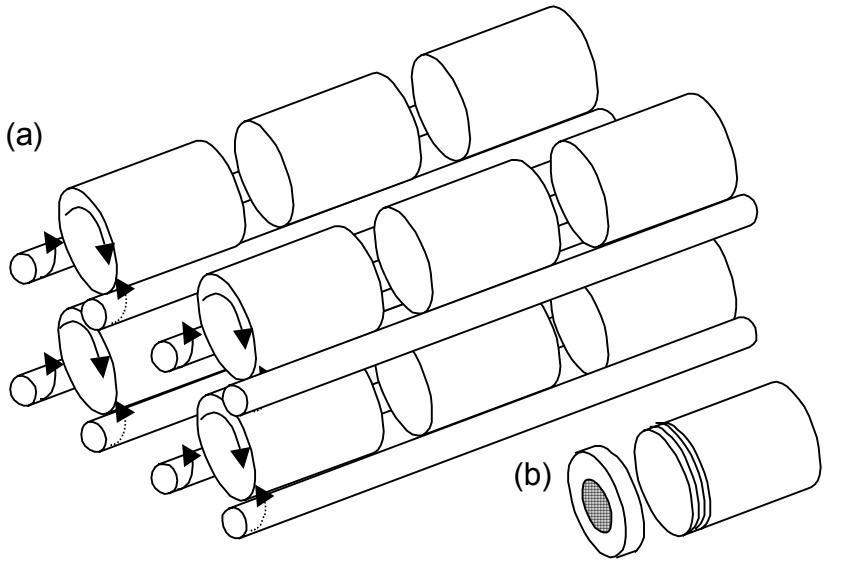

Fig. 8.8. (a) A simple roller bottle system, based on systems used for tissue culture. It is possible to have various layers of roller bars. The system would typically be placed in a temperature-controlled room. For each pair of roller bars that holds several roller bottles, one is a drive bar (*solid arrow*) and the other a slave bar (*dashed arrow*). **(b)** Typically each roller bottle would have a removable lid, with a mesh that allows the exchange of gases

patterns are likely to be complex. The flow patterns within the bed and the headspace of Group III bioreactors have only recently started to be explored. To date, the attention has been largely focused on rotating drum bioreactors. Note that quantitative approaches for determining bed-to-headspace transfer coefficients will be discussed in Sect. 20.5.

8.4.1 Solids Flow Regimes in Rotating Drums

Solids flow in both the radial and axial directions must be considered.

The radial flow regime within the solid bed is important because it affects the heat and mass transfer between the bed and the headspace and the homogeneity within the bed. Transfer of heat, water, and O_2 will be most effective when all substrate particles within the bed are regularly brought to the surface. However, this is not necessarily easy to achieve.

In non-SSF applications of unbaffled rotating drums, the various radial solids flow regimes that occur have been characterized (Fig 8.9). The flow regime depends on several factors, including the rotational rate and the percentage filling of the drum. It is convenient to relate the flow regimes to fractions of the critical rotational speed (N_C), which is defined as the speed at which the particles are held against the inside of the drum wall by centrifugal action (Ishikawa et al. 1980).

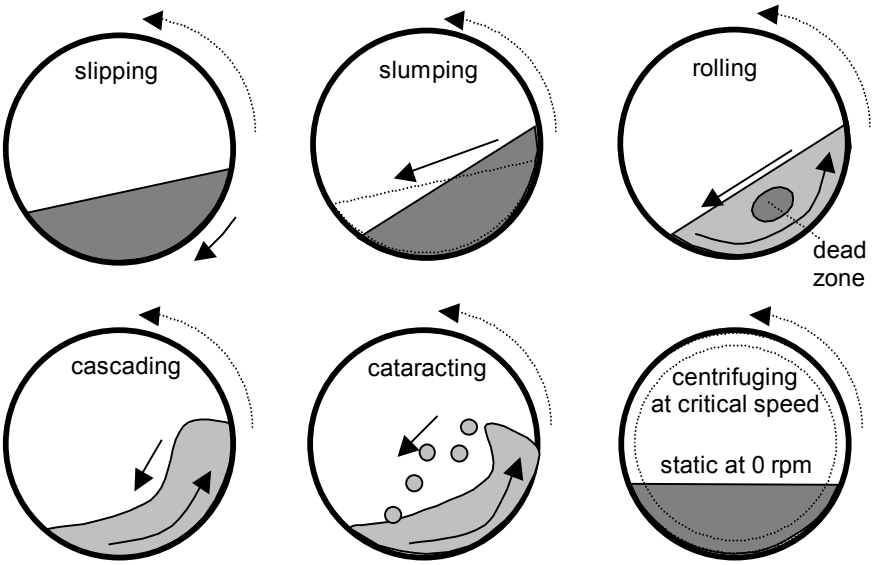

Fig. 8.9. Solids flow patterns within rotating drums without baffles. Relatively slow rotational rates are commonly used in SSF with rotating-drum bioreactors, giving the slumping flow regime. The *darker color* indicates poorly mixed parts of beds while the *lighter color* indicates better-mixed areas. *Solid arrows* indicate movement of the bed or particles within the bed. Adapted from Wightman and Muzzio (1998), with kind permission of Elsevier

This is a function of the drum diameter and for a horizontal drum is given by the following equation:

$$N_C = \frac{42.3}{\sqrt{D}} \tag{8.1}$$

where N_C is in rpm and D is the drum diameter in meters.

For both a static drum (0 rpm) and a drum rotating at the critical speed, there is no mixing action within the bed. For the slipping and slumping flow regimes, which occur when the rotational rate is less than 10% of the critical rotational speed, the bed moves essentially as a whole, meaning that the amount of mixing within the bed itself is negligible.

As the rotational speed increases through moderate rotational rates (from 10% to 60% of the critical rotational speed) the bed undergoes first rolling flow, characterized by a flat surface, and then cascading flow, characterized by a curved surface. There are no airborne particles. In both these flow regimes there is particle flow within the bed itself, although there may be dead zones. For rotational rates greater than 60% of the critical rotational speed, the flow changes to cataracting flow, in which particles are thrown into the air.

Most rotating-drum bioreactors are operated in conditions that give slumping flow, meaning that it is usually a good idea to attach baffles to the inner surface of the drum, in order to improve the mixing. However, it is also possible to operate

unbaffled drums at high rotation rates. For example, the large-scale rotating-drum bioreactor reported by Ziffer (1988) had a diameter of 1.22 m, which gives a critical rotational speed of 38.3 rpm. During the period of peak growth rate the drum was rotated at 24 rpm, which represents 63% of the critical rotational speed, such that the bed must have been on the borderline between the cascading and cataracting flow regimes.

Schutyser et al. (2001) undertook studies of mixing in rotating drum bioreactors that give a greater insight into the radial mixing patterns that occur and how they are affected by baffles. They used a two-dimensional discrete-particle model, in which the predicted positions of a large number of individual particles are calculated by the model, with the change in the position of each individual particle during a time step depending on the sum of forces acting upon it as a result of collisions with other particles or with solid surfaces such as the bioreactor wall (Fig. 8.10(a)). They supported their modeling work with experimental validation in rotating drums containing cooked wheat grains.

They characterized the drum as being well mixed when the entropy of mixing was greater than 0.9 (see Fig. 8.10(b)) and compared the effectiveness of the mixing provided by a particular mode of drum design and operation on the basis of the number of drum rotations necessary to reach an entropy of mixing of 0.9.

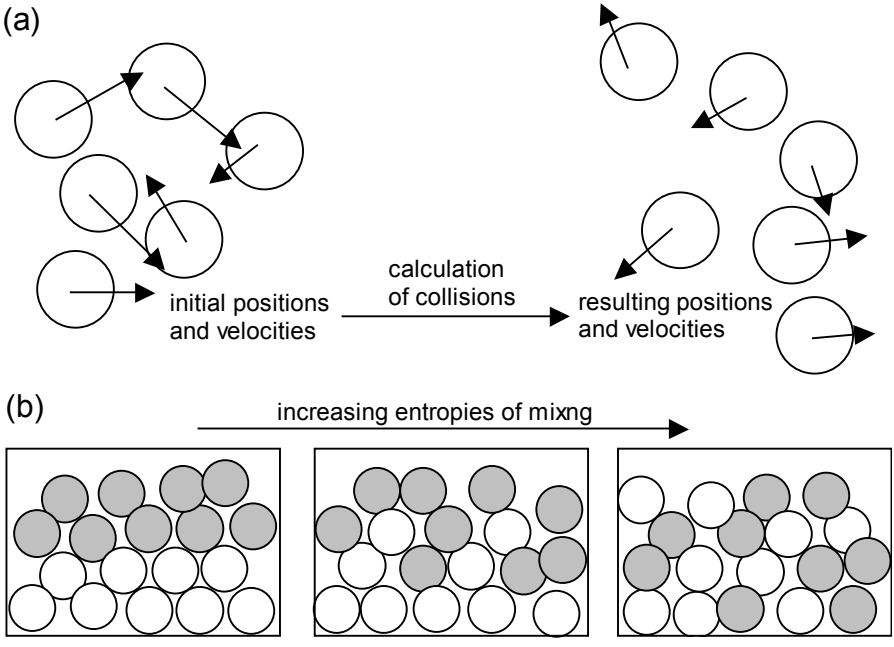

Fig. 8.10. (a) Basis of the discrete-particle modeling work done by Schutyser et al. (2001, 2002). The *arrow* originating from the center of each particle shows its velocity (magnitude and direction). **(b)** Concept of the entropy of mixing. The more random the distribution of particles in relation to their original position, the greater the entropy of mixing

The effects of drum rotational speed (0.5, 2, and 5 rpm), drum diameter (0.15, 0.3, and 1 m) and the fraction of the drum occupied by the bed (0.2, 0.33, and 0.4) were investigated. In the various experiments and simulations, between 1.5 and 10 rotations were necessary in order to reach the well-mixed state. The number of rotations required was essentially independent of the drum rotational speed, although of course for faster speeds the required number of rotations was completed in a shorter time. The effect of drum diameter and fractional filling of the drum were related to their effects on the ratio of the exposed surface area of the bed to the bed volume (R_B, m^{-1}), with the number of rotations required to achieve the well-mixed state initially falling quickly as this ratio increased, reaching a plateau of 1.5 rotations when this ratio had a value of 20 (Fig. 8.11(a)).

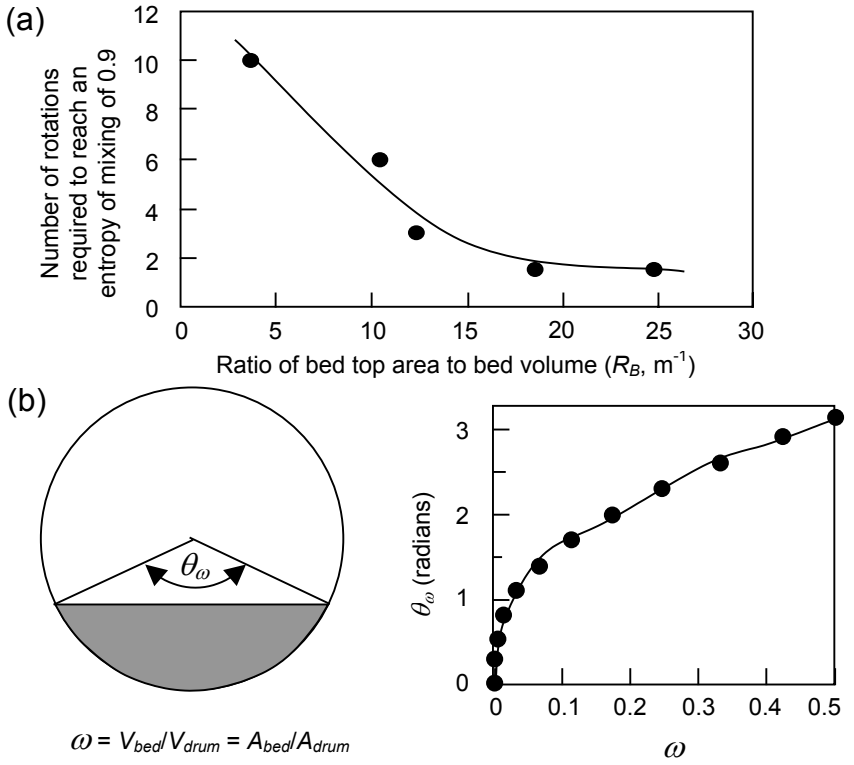

Fig. 8.11. Mixing in an unbaffled rotating drum. **(a)** Dependence of the number of rotations required to reach an entropy of mixing of 0.9 on the ratio of the bed top area to bed volume. The data are from a table presented by Schutyser et al. (2001), adapted with kind permission from John Wiley & Sons, Inc. **(b)** Equation (8.2) is expressed in terms of θ_ω, the angle subtended at the center of the drum by the bed surface, as shown on the left. Note that V and A represent volume and area, respectively. The graph on the right shows θ_ω as a function of the fraction of the drum occupied by the bed, according to Eq. (8.4)

Note that the ratio of exposed surface area to bed volume can be calculated as (Schutyser et al. 2001):

$$R_B = \frac{8}{D}\left(\frac{\sin(\theta_\omega/2)}{\theta_\omega - \sin(\theta_\omega)}\right) \tag{8.2}$$

where D is the drum diameter (m) and θ_ω is the angle in radians subtended at the center by the bed surface for a particular fractional filling ω (m^3-bed m^{-3}-total-bioreactor-volume). Note that θ_ω can be determined from the following relationship:

$$\omega = \left(\frac{\theta_\omega - \sin(\theta_\omega)}{2\pi}\right) \tag{8.3}$$

Unfortunately it is not possible to isolate θ_ω on the left hand side of this equation. However, it is possible to use this equation to plot θ_ω against ω and to fit a polynomial equation. Doing this for values of ω from 0 to 0.5 gives the following explicit equation for θ_ω in terms of ω (Fig. 8.11(b)):

$$\theta_\omega = -3412\omega^6 + 6461.3\omega^5 - 4738.7\omega^4 + 1697.5\omega^3 - 310.36\omega^2 + 31.567\omega + 0.326. \tag{8.4}$$

For unbaffled drums, for a particular fractional filling (ω), Eqs. (8.2) and (8.4) can be used to calculate R_B, which in turn can be compared against Fig. 8.11(a) in order to evaluate the effectiveness of radial mixing that can be expected.

Schutyser et al. (2001) did simulations to investigate the degree to which baffles affect mixing. They compared baffles of 5 cm and 10 cm width within a 30 cm diameter drum, fitting four straight baffles around the inner circumference of the drum (in the manner shown in Fig. 8.1). The smaller baffles had little effect in increasing mixing in the tumbling regime, although at low rotation rates they helped to prevent slumping flow. The larger baffles did improve the effectiveness of mixing.

Schutyser et al. (2002) extended the discrete-particle modeling approach to three dimensions and used it to analyze radial and axial mixing in three different drum designs: a drum without baffles, a drum with four straight baffles (each with a width of 66% of the drum radius) and curved baffles. Straight large baffles do increase axial mixing compared to that in an unbaffled drum, even though they are not designed specifically to push substrate along the axis of the drum. Schutyser et al. (2002) attributed this effect to the higher particle velocities that occur at the surface of the bed. The best design for good axial and radial mixing is a drum with curved baffles, in which the substrate is well mixed axially after three to four rotations. In the same drum without baffles, it can require of the order of 50 to 100 rotations for the bed to be well mixed in the axial direction. Schutyser et al. (2002) noted that with curved baffles it is interesting to incline the central axis of the drum (Fig. 8.12). It can be inclined up until the dynamic angle of repose of the solid, which in their case was 35°, although they suggested that 20° might be more appropriate.

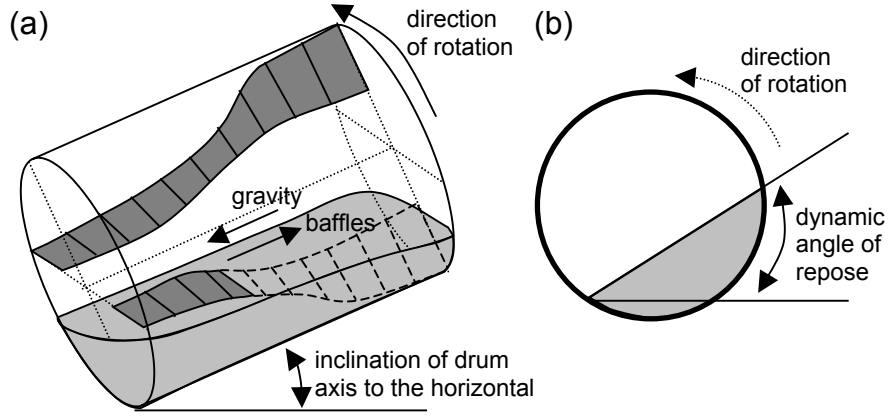

Fig. 8.12. (a) The use of angled baffles and an inclined axis in order to promote axial mixing within a rotating drum bioreactor (Schutyser et al. 2002). Only two baffles are shown, but more can be fitted. **(b)** The dynamic angle of repose of an agitated bed of solids, which represents an upper limit on the inclination of the drum axis that should be used. Adapted from Schutyser et al. (2002) with kind permission from John Wiley & Sons, Inc.

8.4.2 Gas Flow Regimes in the Headspaces of Rotating Drums

The necessity of knowing the headspace flow patterns in order to calculate bed-to-headspace exchange can be seen by using convective heat exchange as an example, although the argument also applies to exchange of O_2 and water. Convective heat removal to the headspace gases (R_{conv}, W) is described as follows:

$$R_{conv} = hA(T_{bed} - T_{head}) \tag{8.5}$$

where h is the heat transfer coefficient (W m^{-2} $°C^{-1}$), A is the contact area between the bed and the headspace, T_{bed} is the bed temperature, and T_{head} is the headspace gas temperature. It is assumed that the bed is well mixed. As shown in Fig. 8.13, if the headspace is well mixed, then the driving force for heat transfer is constant, and the rate of heat transfer is the same at each location on the bed surface. On the other hand, if the flow through the headspace follows the plug-flow regime, then the driving force for heat transfer decreases as the gas heats up as it flows through the drum. In this case the rate of heat exchange between the bed and the headspace is greater near the inlet end of the drum than near the outlet end.

Some studies of headspace flow patterns have been undertaken. Stuart (1996) used a drum of 19 cm internal diameter by 85 cm length that was initially aerated with air and then a 5-minute pulse of pure N_2 was introduced. The outlet O_2 concentration was monitored with a paramagnetic O_2 analyzer and the shape of the response curve was compared with curves that would be expected for several theoretical flow regimes. She studied the effects of two flow rates (2.7 and 5.0 L min^{-1}) three substrate loadings (0, 1, and 2 kg of wheat bran substrate) and 4 rotational speeds (0, 5, 10, and 50 rpm).

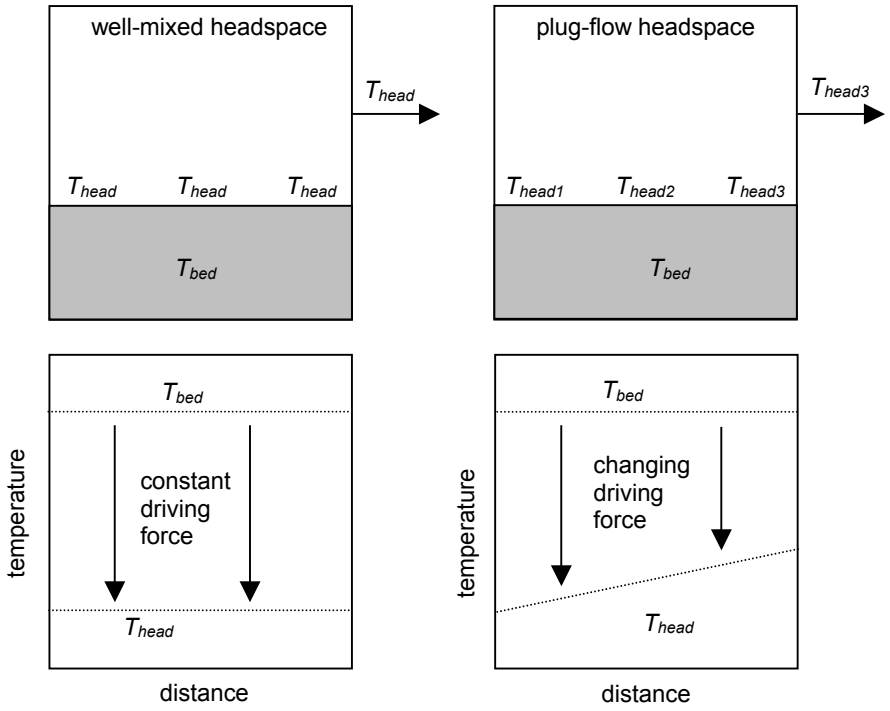

Fig. 8.13. The importance of the headspace flow patterns in affecting bed-to-headspace heat and mass transfer. Two extreme cases are shown. In both cases it is assumed that the bed is well mixed. **(a)** If the headspace is well mixed, then the driving force for heat transfer is equal at all axial positions **(b)** If the flow through the headspace occurs by plug flow, then the driving force for heat transfer decreases as the air flows past the bed surface

In some cases the curves were consistent with a flow regime consisting of several well-stirred regions in series (Fig. 8.14(a)). In other cases they were consistent with plug-flow with axial dispersion (Fig. 8.14(b)). The rotational speed did not affect the type of headspace flow regime. Drums without substrate gave patterns at both gas flow rates that were consistent with the presence of 1 to 2 well-mixed regions in series within the headspace. However, in the presence of substrate there was a difference between the flow patterns at the two different gas flow rates. At both substrate loadings, the response curves obtained with the gas flow rate of 2.7 L min^{-1} were consistent with the presence of 1 to 3 well-mixed regions in series within the headspace, whereas the response curves obtained with the gas flow rate of 2.7 L min^{-1} were consistent with plug-flow with axial dispersion.

Hardin et al. (2001) used CO as a tracer to study flow patterns in a 200-L drum. The patterns were consistent with those that would be expected for a central plug-flow region surrounded by a dead region (Fig. 8.15(a)). The dead region includes a part of the headspace gases and all of gas in the inter-particle spaces in the bed. The dead region is well mixed in the radial direction but there is no axial transport.

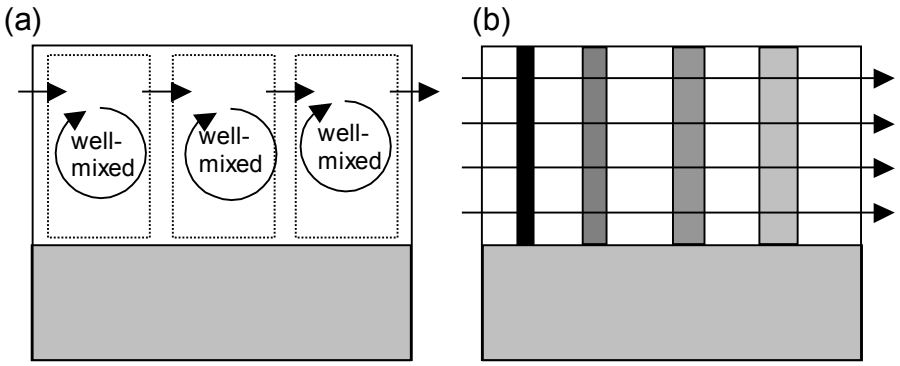

Fig. 8.14. In various different conditions, the residence time distribution patterns for gas flow in the headspace of a rotating drum followed either **(a)** a pattern consistent with several well-mixed regions in series or **(b)** plug flow with axial dispersion (Stuart 1996)

The presence or absence of baffles and the superficial velocity had the greatest effects on the fraction of the drum occupied by the dead region and the rate of transfer between the plug-flow and dead regions (Fig. 8.15(b)). With an increase in the superficial velocity of the air (defined as the volumetric air flow rate divided by the cross-sectional area of the empty drum) there was less mixing between the plug-flow and dead regions and the dead region occupied a greater proportion of the gas volume in the drum. Compared to the absence of lifters, the presence of lifters led to a greater degree of exchange between the plug-flow and dead regions and meant that the dead region represented a smaller proportion of the drum.

Unfortunately, it is not possible to make generalizations from these studies. Flow patterns within the headspace of rotating-drum bioreactors will be greatly influenced by the design and positioning of the air inlet and outlet. One thing is clear, however: If end-to-end aeration is used, it is not reasonable to assume that the headspace is well mixed.

8.5 Conclusions on Rotating-Drum and Stirred-Drum Bioreactors

The following conclusions can be made about the design and operation of rotating-drum and stirred-drum bioreactors on the basis of the experimental work reported above:

- If a rotating-drum bioreactor is used, a decision needs to be made about the rotational rate. If a rotational rate greater than 10% of the critical speed is to be used, then it may not be essential to include baffles within the drum. However, it will require large power inputs to maintain the high rotation rate. The other option is to use quite low rotation rates but to baffle the drum in order to promote mixing.

- End-to-end mixing should be promoted by using curved baffles and inclining the drum axis. Our knowledge is not sufficient to allow detailed advice on the best way of designing curved baffles but obviously the inclination of the central axis must not be greater than the dynamic angle of repose of the solids.
- Discontinuous rotation of the drum or agitator will probably be of little benefit at large scale. Discontinuous rotation brings the added disadvantage of having to overcome inertia, both when starting and when stopping rotation.

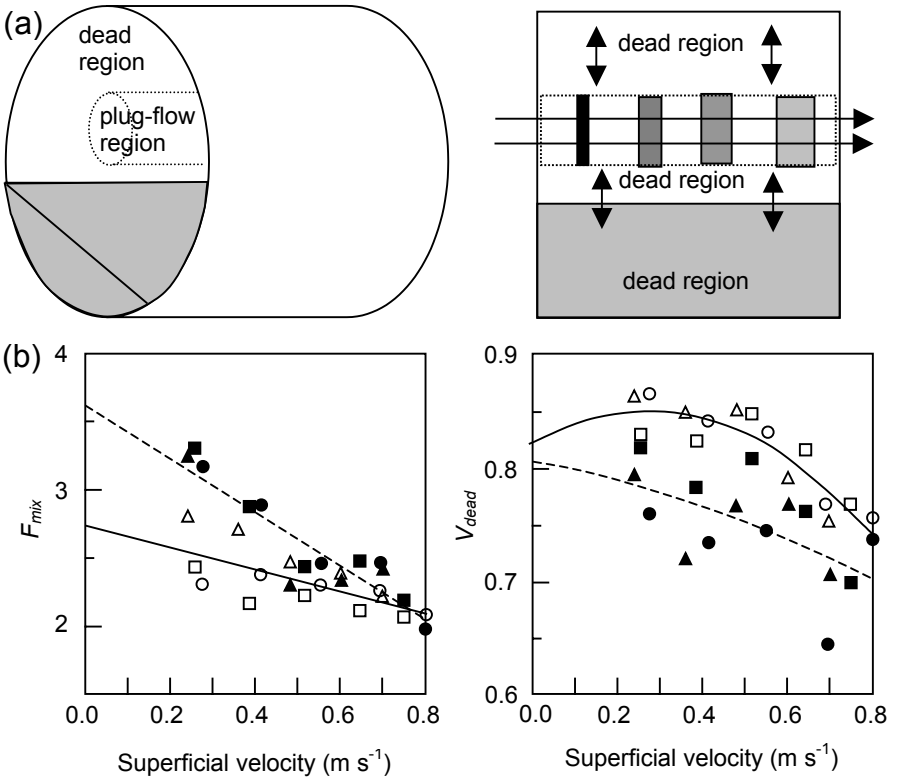

Fig. 8.15. Results of the residence time distribution studies of Hardin et al. (2001). **(a)** A descriptive model consistent with their results. **(b)** Effect of the superficial velocity, baffles, and fill depth on the exchange between the plug-flow and dead regions (characterized by the dimensionless variable F_{mix}) and the volume of the dead region (characterized by the dimensionless variable V_{dead}). F_{mix} is the volumetric exchange rate between the dead and plug-flow regions relative to the volume of the drum and the mean residence time, such that a F_{mix} of 1 would be equal to one volume of the drum exchanged per mean residence time. V_{dead} is the volume of the dead region relative to the total volume of the gas inside the drum. Key: *Hollow symbols* and *solid lines* represent an unbaffled drum. *Solid symbols* and *dashed lines* represent a baffled drum. The *circles* represent 26% filling, the *triangles* 19.5% filling and the *squares* 13% filling. Adapted from Hardin et al. (2001), with kind permission from John Wiley & Sons, Inc.

- Fractional fillings should not be more than 0.4 and may need to be less. In fact, the optimal fractional filling, that is, the filling that allows you to use as much of the drum volume as possible without compromising mixing too much, must be determined experimentally for each particular combination of substrate and microorganism.
- Our knowledge is not sufficient to allow detailed advice on the best design of mixers in the case of stirred-drum bioreactors.

Further Reading

Studies of heat and mass transfer in rotating-drum bioreactors

Fung CJ, Mitchell DA (1995) Baffles increase performance of solid-state fermentation in rotating drums. Biotechnol Techniques 9:295–298

Hardin MT, Howes T, Mitchell DA (2001). Residence time distribuition of gas flowing through rotating drum bioreactors. Biotechnol Bioeng 74:145–153

Hardin MT, Howes T, Mitchell DA (2002) Mass transfer correlations for rotating drum bioreactors. J Biotechnol 97:89–101

Schutyser MAI, Weber FJ, Briels WJ, Rinzema A, Boom RM (2003) Heat and water transfer in a rotating drum containing solid substrate particles. Biotechnol Bioeng 82:552–563

Selected examples of studies undertaken in rotating-drum bioreactors

Kalogeris E, Iniotaki F, Topakas E, Christakopoulos P, Kekos D, Macris BJ (2003) Performance of an intermittent agitation rotating drum type bioreactor for solid-state fermentation of wheat straw. Bioresource Technol 86:207–213

Kargi F, Curme JA (1985) Solid-state fermentation of sweet sorghum to ethanol in a rotary-drum fermenter. Biotechnol Bioeng 27:1122–1125

Marsh AJ, Mitchell DA, Stuart DM, Howes T (1998) O_2 uptake during solid-state fermentation in a rotating drum bioreactor. Biotechnol Letters 20:607–611

Mitchell DA, Tongta A, Stuart DM, Krieger N (2002) The potential for establishment of axial temperature profiles during solid-state fermentation in rotating drum bioreactors Biotechnol Bioeng 80:114–122

Stuart DM, Mitchell DA, Johns MR, Litster JD (1998) Solid-state fermentation in rotating drum bioreactors: Operating variables affect performance through their effects on transport phenomena. Biotechnol Bioeng 63:383–391

Simplified approach to making design and operating decisions for rotating drums

Hardin MT, Mitchell DA, Howes T (2000) Approach to designing rotating drum bioreactors for solid-state fermentation on the basis of dimensionless design factors Biotechnol Bioeng 67:274–282